Enhancing Aromatic Production from Reductive Lignin Disassembly: *in situ* O-methylation of Phenolic Intermediates.

Jacob A. Barrett[‡,§], Yu Gao[‡,†], Christopher M. Bernt[§], Megan Chui[§], Anthony T. Tran[§], Marcus B. Foston*[,†], Peter. C. Ford*[,§].

[§]Department of Chemistry and Biochemistry, University of California, Santa Barbara, Santa Barbara, CA, 93106-9510 USA

[†]Department of Energy, Environmental & Chemical Engineering, Washington University in St. Louis, One Brooking Drive, St. Louis, MO. 63130 USA

Email: MBF: mfoston@wustl.edu; PCF: ford@chem.ucsb.edu

KEYWORDS: lignin, heterogeneous catalysis, hydrotalcite, porous metal oxides, supercritical methanol, dimethyl carbonate.

ABSTRACT: The selective conversion of lignin into aromatic compounds has the potential to serve as a "green" alternative to the production of petrochemical aromatics. Herein, we evaluate the addition of dimethyl carbonate (DMC) to a biomass conversion system that uses a Cu-doped porous metal oxide (Cu_{20}PMO) catalyst in supercritical methanol (sc-MeOH) to disassemble lignin with little to no char formation. While Cu_{20}PMO catalyzes C-O hydrogenolysis of aryl-ether bonds linking lignin monomers, it also catalyzes arene methylation and hydrogenation, leading to product proliferation. The MeOH/DMC co-solvent system significantly suppresses arene hydrogenation of the phenolic intermediates responsible for much of the undesirable product diversity via O-methylation of phenolic –OH groups to form more stable aryl-OCH_3 species. Consequently, product proliferation was greatly reduced and aromatic yields greatly enhanced with lignin models, 2-methoxy-4-propylphenol, benzyl phenyl ether, and 2-phenoxy-1-phenylethan-1-ol. In addition, organosolv poplar lignin (OPL) was examined as a substrate in the MeOH/DMC co-solvent system. The products were characterized by nuclear magnetic resonance spectroscopy (^{31}P, ^{13}C, and 2D ^{1}H-^{13}C NMR) and gas chromatography-mass spectrometry techniques. The co-solvent system demonstrated enhanced yields of aromatic products.

INTRODUCTION.

Society's dependence on fossil carbon resources is linked not only to energy needs, but also to demand for chemical feedstocks. Petroleum accounts for ~36 % of annual energy consumption and 95 % of organic chemicals produced in the United States.[1,2] The environmental impact of the resulting anthropogenic CO_2 emissions has motivated interest in sustainable technologies to meet our growing energy and manufacturing demands. In this context, significant activity has focused on developing large-scale bio-refineries that would efficiently utilize lignocellulosic biomass for fuel and chemical production.[3,4]

The lignin component of biomass has potential as a renewable source for industrially useful aromatic chemicals.[5] While technologies for selective conversion of the carbohydrate components of lignocellulosic biomass have been successful,[6] lignin is generally treated as waste and burned for low grade heat. The development of sustainable technologies for converting lignin to aromatic products in high yield, selectivity, and value would improve the economic feasibility and life cycle assessment for 2nd generation (i.e., using lignocellulosic biomass feedstock) fermentative bio-refineries.[7]

Lignin is an aromatic macromolecule that comprises one of the three main components of lignocellulosic biomass, cellulose and hemicellulose being the others.[8] The polymeric structure of lignin results from radical polymerization of three hydroxycinnamyl alcohols: coniferyl alcohol (G), sinapyl alcohol (S), and coumaryl alcohol (H). The resulting macromolecule is naturally recalcitrant to biotic and abiotic degradation. The monomers of lignin are linked through several substructures that contain C-O bonds, in particular aryl ether (β-O-4 and α-O-4), phenylcoumaran (β-5), and diaryl ether (4-O-5) linkages.[8] Other linkages are present in smaller amounts with abundances being highly dependent on the plant species, growth conditions, and lignin isolation technique (Figure 1).[9-11]

Various lignin disassembly methods utilizing acids, bases, and transition metal based hetero- and homogeneous catalysis have been described,[12-16] including catalytic hydrogenolysis to produce aromatic compounds from several types of lignin.[17,18] Hydrogenolysis (HDG) uses hydrogen to cleave C-X (X= O,

S, Cl, and F) bonds.[20] Such reductive cleavage of aryl-ether bonds is a high-potential route towards the production of value-added aromatic products. β-O-4 and α-O-4 linkages generally undergo cleavage by HDG more easily than do other types of lignin bonds.[21] However, catalysts effective for C-O bond HDG often promote unwanted hydrogenation of the arene rings to give cyclohexyl derivatives. A major objective in lignin valorization through HDG is to cleave aryl-ether bonds while minimizing aromatic ring hydrogenation.

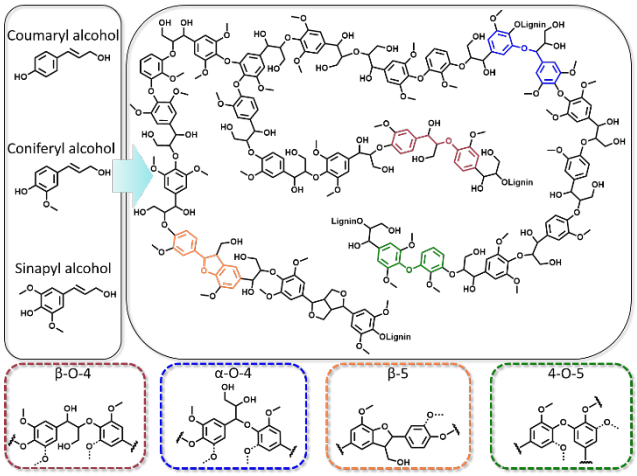

Figure 1. Graphical depiction of lignin based on structural data on poplar wood from Sannigrahi et. al.[8] The three major lignin monomer precursors are depicted on the left with four of the common aryl-ether linkages depicted on the bottom.

Various factors have profound effects on the rates and selectivities of key pathways for lignin disassembly by heterogeneous catalysts. For example, Song et al. observed that the nickel catalyzed HDG of lignosulfonate to organic liquids and the selectivity toward production of propyl guaiacol and 4-ethylguaiacol are dependent on the catalyst support.[22] In another contribution, this group discussed the important role that methanol (MeOH) can play in lignin solvation and solvolysis. Hence, given the limitation of transport between lignin and a heterogeneous catalyst, hydrogenolysis is likely to occur on smaller, soluble lignin fragments generated by solvolysis.[23] An undesired side reaction, owing to high temperatures required for solvolysis to monomers, is formation of intractable tar/char due to condensation pathways.

The catalytic lignin disassembly system developed in our laboratory is based on a copper-doped porous metal oxide catalyst prepared by calcining a 3:1 Mg^{2+}:Al^{3+} hydrotalcite (layered double hydroxide). The synthetic hydrotalcite used here has 20 % of the Mg^{2+} replaced with Cu^{2+} (Cu_{20}HTC) and yields Cu_{20}PMO upon calcination.[24,25] In supercritical methanol (sc-MeOH at 280-320 °C and ~100 bar), Cu_{20}PMO catalyzes the disassembly of lignin, and even lignocellulosic biomass such as milled wood, in a one-pot process with little to no char formation.[26,27] The products are a mixture of aliphatic alcohols. Cu_{20}PMO is uniquely effective in MeOH, catalyzing MeOH reforming and water gas shift reactions that generate the necessary reducing equivalents of H_2 (eqs. 1 & 2). Subsequent studies showed Cu_{20}PMO and related catalysts to be effective in disassembling different types of lignin,[28] producing H_2 equivalents from other alcohols,[29,30] and performing selective organic transformations[31] such as the upgrading of furfural derivatives.[32]

$$CH_3OH \rightleftharpoons 2\,H_2 + CO \qquad (1)$$

$$CO + H_2O \rightleftharpoons CO_2 + H_2 \qquad (2)$$

A key issue with Cu_{20}PMO catalyzed lignin disassembly in sc-MeOH is product proliferation owing to arene hydrogenation and methylation. Our model studies showed that these side reactions can largely be attributed to the reactivity of phenolic intermediates.[33] In contrast, corresponding O-methylated models such as anisole are relatively stable in this catalytic system. In an earlier study, we briefly showed that the introduction of the methylating agent dimethyl carbonate (DMC) greatly enhanced the net yield of aromatic products from the α-O-4 lignin model, benzyl phenyl ether.[33] This enhancement can be attributed to interception of phenol, the anticipated HDG intermediate by O-methylation to give anisole. Notably, O-methylation of guaiacol, catechol, and phenol by DMC has been reported by Jyothi and coworkers to be catalyzed by calcined Mg-Al hydrotalcite.[34,35]

The present study applies this methodology to stabilize or trap reactive phenolic intermediates generated during the reductive disassembly of lignin and of several relevant models. We describe studies with several lignin model compounds including 2-phenoxy-1-phenylethan-1-ol, which is a model for the β-O-4 linkage that comprises 40-60 % of lignin's linkages,[8] and with organosolv poplar lignin (OPL), which is a much more complex model for lignins. These results each show substantially higher yields of aromatic products in the MeOH/DMC co-solvent system (vs. reaction in sc-MeOH).

EXPERIMENTAL SECTION.

Materials. Methanol was purchased from Fischer Scientific and dried using molecular sieves (type 3 Å 8-12 mesh beads). Acetone, K_2CO_3, and ethanol were used as purchased from Fischer Scientific. Dimethyl carbonate, synthetic hydrotalcite, n-decane, phenol, 2-bromoacetophenone, and 2-methoxy-4-propylphenol (MPP) were used as purchased from Sigma Aldrich. Benzyl phenyl ether (BPE) was used as purchased from Acros Organics. Diphenyl ether (DPE) and dihydrobenzofuran (DHBF) were purchased from Oakwood Chemicals and used as received. 2-Phenoxy-1-phenylethan-1-ol (PPE) was synthesized according to a known procedure.[36] Further details and characterization can be found in the Supporting Information (SI). Organosolv poplar lignin (OPL) was obtained by treatment of poplar wood chips using an adaptation of a previous procedure, also further described in the SI. NMR characterization showed no significant carbohydrate in these samples.[37]

Catalyst synthesis and characterization. Copper-doped hydrotalcite (Cu_{20}HTC) was prepared by the standard co-precipitation method[24,25] and analyzed by inductively coupled plasma atomic emission spectroscopy (ICP-AES), powder-x-ray diffraction (XRD) and attenuated total reflectance IR spectroscopy as described in the SI (Figure S1) The observed Cu/Mg/Al ratio of 0.62/2.48/1.0 was consistent with the molecular formula $Cu_{1.2}Mg_{4.8}Al_2CO_3(OH)_{16}{\cdot}4(H_2O)$. Cu_{20}HTC was calcined at 460 °C for 15 h to obtain Cu_{20}PMO, which

was shown to have a BET surface area of 158 m^2/g consistent with previous reports.

All ICP-AES measurements were obtained using a ThermoiCAP 6300 ICP equipped with a 6000 K Ar plasma. Powder XRD patterns were collected under ambient temperature using a Panalytical Empyrean Diffractometer, with Cu Kα radiation (λ= 1.5405980 Å) in a stainless steel sample holder, scanned from 5-75° (2θ). Structures were assigned using a reference or crystal structure database.[38] ATR-IR spectra were collected on a Bruker ALPHA FT-IR instrument.

Batch reactions. Small-scale reactions were conducted using custom built, high-pressure stainless steel reactors. The mini-autoclave reactors consisted of a 3/4 Swagelock union with two 3/4 inch Swagelock plugs and have an internal volume of ~10 mL. These are described in detail in Matson et al.[22] A typical catalysis run consisted of a set of mini-reactors charged identically with a substrate, catalyst, methanol (2-3 mL), dimethyl carbonate (0-1 mL), and an internal standard n-decane (20 µL). With model compounds, the substrate sample was 0.25 to 1 mmol, and a 50 mg portion of catalyst was used. For studies with OPL, the sample size was 100 mg and a 100 mg portion of catalyst was used. Temporal product distribution studies were conducted by adding identical quantities of substrate, catalyst, and solvent to a set of mini reactors. These reactors were sealed and placed in an aluminum heating block in a preheated oven set at a specified temperature (typically 300 ºC). Individual reactors were removed after a given time interval (1-6 hours) and quenched via rapid cooling in a water bath. The volume of the gas phase was measured with a water displacement apparatus containing a 1/4 inch brass Swagelock pipe tee fitted with a septum for gas analysis samples. (WARNING: High pressures are produced from the reactions and appropriate precautions should be taken when handling and opening.) The reactors were washed with methanol and the combined liquids were filtered using a 10 mL syringe fitted with a 0.2 µm Acrodisc nylon membrane filter.

Analysis of products from model reactions. Product identification and quantification was largely done by gas chromatography with thermal conductivity, flame ionization, and mass spectrometry detection (GC-TCD, GC-FID, and GC-MS, respectively). Details on the specifics of the GC methods are described in the SI. Gas phase products (H_2, CO, CH_4, and CO_2) were quantified by comparison to calibration curves generated using a standardized syngas mixture. Liquid products were quantified using response factors (rf) for all analytes that were approximated using the effective carbon number (ECN) technique described previously,[33] based upon work by Scanlon and Willis (see SI).[39]

Kinetics analysis. Reactions were assumed to be first order with respect to the reactant at each step. Global fitting was performed using DynaFit version 4.05.087 software on a desktop computer (BioKin Ltd.) as described previously.[35]

Characterization of disassembled lignin. The products of the OPL disassembly with Cu_{20}PMO under various reaction conditions were characterized by GC-MS, gel permeation chromatography (GPC), and NMR (^{31}P, ^{13}C, and 2D ^{1}H-^{13}C) spectroscopy. Further details are described in the SI.

GC-MS analysis of disassembled lignin was carried out on an Agilent GC system 7890A coupled with Agilent 5975C mass spectrometry with triple-axis detector. The data were analyzed through ChemStation Software. Compounds were identified by comparing their mass spectra with those from the system database (NIST10). The weight average molecular weight (M_w), number average molecular weight (M_n), and molecular weight polydispersity of the disassembled and starting lignin were determined by GPC. Unprocessed products were directly injected into the GC-MS and GPC for characterization.

For the NMR analyses of OPL products, the solvent in the product mixtures from lignin disassembly was removed under reduced pressure (~0.3 Torr at ~-20 °C (ice and salt bath) for 24 h) and the volatiles were captured in a liquid nitrogen trap. The resulting oily non-volatile product was then weighed. Samples of the untreated OPL and non-volatile product mixtures were added to separate dry 2-dram vials, followed by the addition of 400 µL DMSO-d_6. The mixtures were stirred under dry N_2 for several hours until completely dissolved, and then transferred into separate NMR tubes.

RESULTS AND DISCUSSION.

Phenol reactivity in MeOH/DMC. Previously, we compared the activity of Cu_{20}PMO with BPE in sc-MeOH with that in MeOH/DMC under conditions effective for disassembly of lignin and lignocellulose.[33] In both solvent systems, the benzyl ether bond undergoes rapid HDG to give toluene and phenol. Toluene is unreactive toward arene hydrogenation or methylation in either medium. The other primary product phenol represents the core chemical moiety of the *p*-hydroxyphenyl (i.e., coumaryl alcohol) monolignol. This phenol product undergoes secondary reactions in sc-MeOH to generate numerous products, mostly aliphatic alcohols. These secondary products are largely attributed to hydrogenation to cyclohexanol, which further reacts to form methylcyclohexanols. In the MeOH/DMC co-solvent, the behavior was significantly different owing to the phenol intermediate undergoing O-methylation to anisole (i.e., methoxybenzene). This was confirmed by studying phenol directly as a substrate in the MeOH/DMC co-solvent. The data presented in SI Table S1 show an 87 % yield of anisole after 6 h reaction at 300 °C. Aliphatic products total only about 5 % (Scheme 1), and ring methylated aromatics make up the remainder. Under these conditions anisole does undergo some hydrodeoxygenation (HDO) to benzene, but the reaction is quite slow. The ring-methylation product, *o*-cresol, was previously shown to convert to xylenol, methylcyclohexanol, and methylanisole in sc-MeOH.[33]

One rationale for the high reactivity of phenol compared to anisole is the difference in interactions with the catalyst surface. Porous metal oxides prepared from transition metal hydrotalcites are solid bases as evidenced by their ability to catalyze trans-esterification reactions of triglyceride.[25] Thus, these catalyst supports should have a greater affinity for an acid substrate like phenol than a neutral compound such as anisole. Similarly, studies of SiO_2-Al_2O_3 surfaces show a much lower molar adsorptivity for anisole than for phenol at 400 °C.[41]

Scheme 1. Reactivity network for phenol[a] in MeOH/DMC with Cu_{20}PMO at 300 °C.

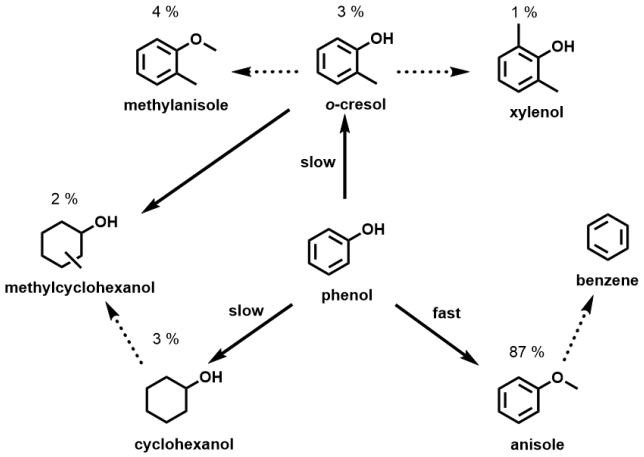

[a]Data for triplicate 6 h runs (SI Table S1).

Reactivity of 2-methoxy-4-propylphenol (MPP). MPP is a more complex model for lignin disassembly intermediates than is phenol (Scheme 2). Two monolignols, guaiacyl (G, or i.e., coniferyl alcohol) and syringyl (S, or i.e., sinapyl alcohol), contain methoxy (-OCH_3) groups. G monomers have one methoxy while S monomers have two. In both monomers, the -OCH_3 functionalities are *ortho* to the phenolic -OH (Figure 1). In this context, we examined MPP reactivity with Cu_{20}PMO in sc-MeOH and in MeOH/DMC at 300 °C. Reaction for 6 h in the sc-MeOH system led to ~50 % conversion of MPP to a broad distribution of products; some were too low in abundance to identify (SI Table S2).

Scheme 2. Observed products from the reaction of MPP[a] in MeOH/DMC with Cu_{20}PMO at 300 °C.

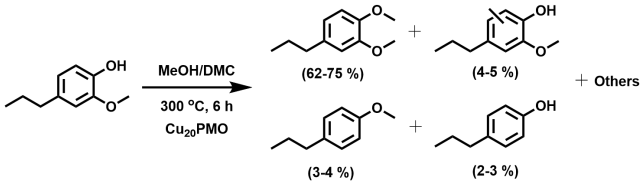

[a]Data for triplicate 6 h runs (SI Table S2).

The largest component of the sc-MeOH product mixture was the O-methylated MPP derivative 1,2-dimethoxy-4-propylbenzene, which represented 21 % of the products. In the MeOH/DMC co-solvent, there was 95 % conversion and better material balance. Not surprisingly 1,2-dimethoxy-4-propylbenzene (67 % yield) was by far the predominant product; however, small amounts of the two HDO products 4-propylphenol and 4-propylanisol were also observed (Scheme 2). (Note: The good material balances from these GC-FID analyses are consistent with the absence of chars or of undetected gaseous products with these model compounds.)

Reactivity of the α-O-4 model, benzyl phenyl ether (BPE). Although the reaction of BPE with Cu_{20}PMO in the presence of DMC was described briefly in an earlier publication,[33] the detailed studies here provide a more comprehensive picture. The temporal distribution of products from the reaction of BPE over Cu_{20}PMO in MeOH/DMC at 300 °C is shown in Figure 2. A complete product list is summarized in SI Table S3 and reaction network in SI Scheme S1. Within 2 h, BPE is entirely consumed, and toluene yield from HDG of the $PhCH_2$-OPh bond is (within experimental uncertainty) quantitative. There is little decay of this product over the next 4 h. The yield of anisole after 2 h, presumably by O-methylation of intermediate phenol is 71 %. Anisole is also relatively unreactive but undergoes a gradual decrease in the yield over the next 4 h. By contrast when the catalysis was carried out in sc-MeOH alone, the yield of toluene was comparable, but the principal oxygen containing products were methylcyclohexanols (72 % yield, SI Table S3). Reducing the DMC used in the co-solvent system (0.5 mL instead of 1 mL to give a 5/1 MeOH/DMC ratio) led to a lower yield of anisole and higher yield of aliphatics (SI Table S6).

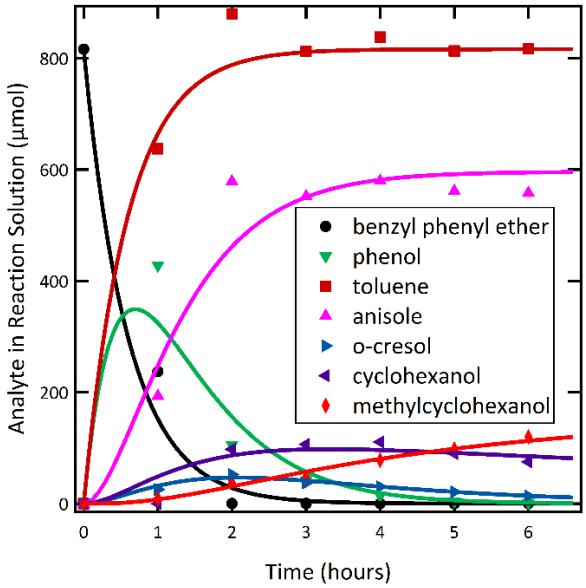

Figure 2. Temporal product distribution from reaction of BPE (~800 µmol) in MeOH/DMC with Cu_{20}PMO (50 mg) at 300 °C. Minor products are listed in SI Table S3.

O-methylation of phenols by DMC results not only in the formation of the stable $ArOCH_3$ species but also in release of MeOH and CO_2. Thus, analysis of the gas phase generated by the reaction of BPE in MeOH/DMC with Cu_{20}PMO at 300 °C shows significantly more CO_2 production than seen in sc-MeOH (SI Tables S4 & S5, SI Figure S2). Notably, over the course of 6 h, the CO_2 initially formed diminishes with a corresponding increase of CO in the gas phase. This may be the result of reverse water gas shift owing to the H_2 generated by Cu_{20}PMO reforming of MeOH.

As Song et al. noted,[22,23] the medium very likely plays a role in the solvolysis of lignin ether linkages to generate lower molecular weight and soluble fragments. One can easily envision such pathways for the α-O-4 linkage of BPE. To address this question, we studied BPE reactivity in sc-MeOH and MeOH/DMC absent the Cu_{20}PMO catalyst. In sc-MeOH at 300 °C, BPE underwent about 23% conversion after 3 h and 51% conversion after 6 h with respective material balances of 89 and 79 % (Table S7). The identifiable products were mostly toluene and phenol, although other products, such as benzo-

phenone and 2-phenylmethylphenol, were seen. The material balance progressively worsened as the reaction proceeded owing to formation of insoluble, presumably polymeric, materials. This compares to the 74% conversion after 1 h and ~100% conversion after 3 h under comparable conditions when the Cu_{20}PMO catalyst is present (material balance ~100%). These observations illustrate the role of the catalyst not only in activating the ether linkage toward HDG but also in preventing char formation by intercepting intermediates that can undergo condensation. When the analogous catalyst-free reaction of BPE was carried out in the MeOH/DMC, conversion was only ~43 % after 6 h. Toluene and phenol were the most prominent products, but, unlike the reaction in sc-MeOH, anisole was also observed. The material balance was ~90 % (SI Table S8).

Another question is whether the metal oxide support itself will catalyze these transformations. When the BPE reaction was studied in sc-MeOH/DMC at 300 °C with copper-free PMO (50 mg) derived from calcining 3:1 Mg-Al hydrotalcite, the conversion was 32 % after 6 h. The four most prominent products were toluene, benzophenone, phenol, and anisole (SI Table S9). The material balance improved somewhat to ~96 %. Although there was some shift in the product distribution, the copper-free PMO was not significantly more active than the catalyst-free systems.

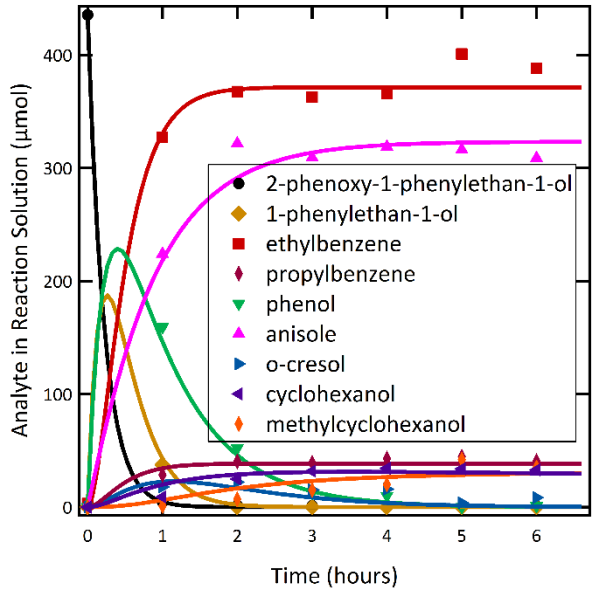

Figure 3. Temporal product distribution from the reaction of PPE (~500 µmol) in MeOH/DMC with Cu_{20}PMO (50 mg) at 300 °C. Additional products are listed in SI Table S10.

Reactivity of the β-O-4 model 2-phenoxy-1-phenylethan-1-ol (PPE). Figure 3 summarizes the temporal evolution of PPE and the products for reaction with Cu_{20}PMO in the MeOH/DMC co-solvent at 300 °C. The β-O-4 bond was cleaved with 98 % conversion in 1 h. A small amount of the expected 1-phenylethanol was observed at 1 h, but this apparently underwent rapid HDO to ethylbenzene (76-92 % yield). Propylbenzene (6-10 % yield, SI Table S10) was a lesser product and can be attributed to β-carbon methylation of 1-phenylethanol followed by HDO.[33] Anisole was also formed (74 % yield after 2 h) and, as noted above, underwent modest decay over longer reaction times. After 3 h, aromatic products represented ~91 % of the theoretical yield. At 6 h the aromatic yield was the same, although there was some redistribution of the products. The aliphatics were mostly cyclohexanols; the remainder was cyclohexanes. Of those products originating from the phenol fraction, the aromatic yields were 89 % and 83 % respectively at 3 h and 6 h. Material balance for each time point was ~100%.

Table S10 also summarizes products and yields from the analogous PPE reactions catalyzed by Cu_{20}PMO in sc-MeOH at 300 °C. In comparison to the MeOH/DMC system, the total yield of aromatic products after 6 h was only 69 %, mostly ethylbenzene and propylbenzene. Of the products originating with the phenol fraction, the aromatic yield was only 33%.

Scheme 3. Reactivity network from the reaction of PPE in MeOH/DMC with Cu_{20}PMO.[a]

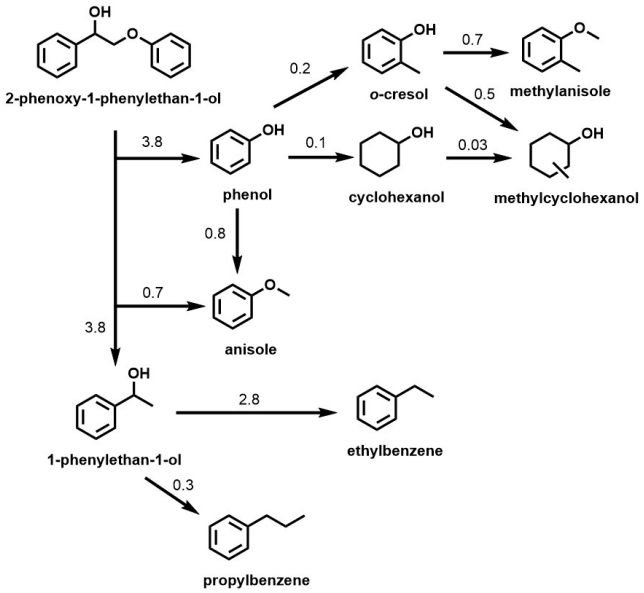

[a]For the calculated rate constants (k_{obs}) the units are h^{-1}.

Scheme 3 also presents the results of a Dynafit analysis of the temporal data shown in SI Table S10 and Figure 3 to estimate rate constants for respective reaction network pathways for PPE in the MeOH/DMC co-solvent. Unlike BPE (SI Scheme S1), the results of the kinetics fitting imply a direct pathway from PPE to anisole. Similar fits were reported in our previous studies of reactivities in sc-MeOH. Comparisons of key reactions such as aryl-ether HDG indicate that these rates are essentially the same in the two solvent systems.

The concentrations of MeOH and DMC affect the overall rate as they serve both as reagents and solvents. Additionally, the CO_2 byproduct from the O-methylation by DMC potentially plays a role in decreasing arene hydrogenation rates by consuming H_2 in the reverse water gas shift reaction. In this context, future studies will explore the possible effect of increasing CO_2 partial pressure as a strategy for limiting arene hydrogenation in reductive lignin disassembly.

Diphenyl ether and 2,3-dihydrobenzofuran. Diphenyl ether (DPE) is a model for the 4-O-5 linkage in lignins while

2,3-dihydrobenzofuran (DHBF) contains β-5 and α-O-4 type linkages (Figure 4). The 4-O-5 and β-5 are common to softwoods such as pine but are less prevalent in hardwoods such as poplar.[12] The 4-O-5 and β-5 linkages are more resistant to cleavage than the α-O-4 and β-O-4 links**,** and this is consistent with the current results. For example, reaction of DPE with Cu_{20}PMO in sc-MeOH or in MeOH/DMC at 300 °C for a period of 6 h, led to relatively little conversion (15% and 7%, respectively) in either medium (SI Table S11).

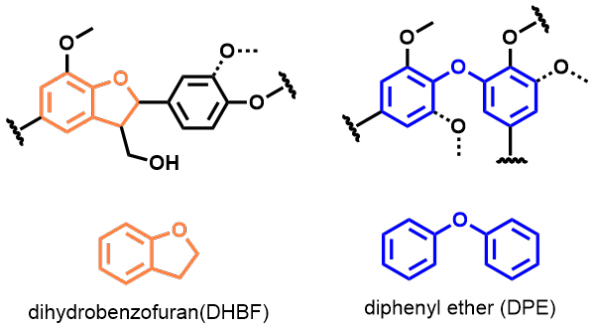

Figure 4. Structures of the β-5 model dihydrobenzofuran and the 4-O-5 model diphenyl ether.

DHBF proved to be more reactive than DPE in the presence of Cu_{20}PMO. After 6 h, the conversion was 57 % in sc-MeOH but only 27 % in MeOH/DMC (SI Table S12). (The respective material balances were 90 % and ~100 %.) However, the products were consistent with those expected from cleavage of the α-O-4 linkage; ethoxybenzene, the expected product of β-5 HDG, was not observed. Although the reactivity of DHBF was lower in MeOH/DMC, a larger percentage of the product was aromatic (73%) than in sc-MeOH (29 %). However, it is not entirely clear why this was so, since the O-methylated product ethyl anisole was a relatively minor product in the former.

Catalytic disassembly of organosolv poplar lignin (OPL). The substrate OPL was examined to assess whether (and how) the conclusions formed on the above model systems inform our understanding of a more complex model for lignin conversion. OPL disassembly was performed by Cu_{20}PMO at 300 °C for 3 h. In sc-MeOH this presumably occurs by solvolysis to give lower molecular weight fragments.[43] Solubilized lignin fragments then undergo HDG in the presence of Cu_{20}PMO (Scheme 4).

Scheme 4. Proposed mechanism of lignin disassembly in MeOH/DMC as catalyzed by Cu_{20}PMO.

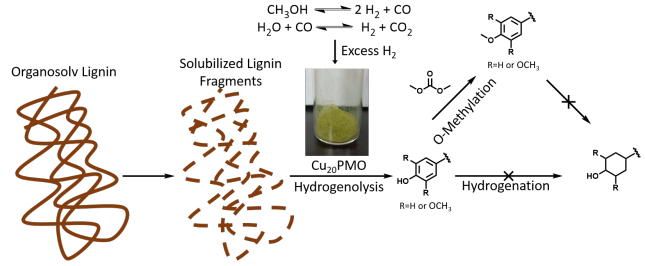

The term "unprocessed" product will refer to liquid samples collected from the reaction while "non-volatile" product will refer to liquid samples from which the solvent was removed under vacuum at ~-20 °C. The weight percent of the recovered non-volatile product from OPL disassembly by Cu_{20}PMO was 45 wt % in sc-MeOH and 64 wt % in MeOH/DMC. In the absence of catalyst, considerable char formation was observed in each medium (35 and 32 wt %, respectively, SI Table S13). No char was observed when the catalyst was present. Similar to the reactions with lignin model compounds, more CO_2 and less H_2 were generated for reactions in MeOH/DMC compared to those in sc-MeOH.

GPC analysis was performed on untreated OPL as well as unprocessed and non-volatile products generated in sc-MeOH and in MeOH/DMC with and without Cu_{20}PMO at 3 h. There was only a modest difference between the chromatographs for the unprocessed and non-volatile products (the latter being slightly higher), meaning that the product molecular weight distributions were not seriously affected by the solvent removal step. Relative molecular weight values including number average molecular weight (M_n), weight average molecular weight (M_w), and polydispersity index (PDI = M_w/M_n) were determined based on a polystyrene standard calibration curve. These data are summarized in SI Table S13. The high PDI for all samples indicates a broad distribution of molecular weights. However, the M_n for each depolymerized sample (~310-390 g/mol) is ~3-4 times lower than that of untreated OPL (~1,290 g/mol). The M_w is considerably larger for products from reactions without Cu_{20}PMO (630-720 g/mol) than from reactions with catalyst (400-510 g/mol) (Figure 5).

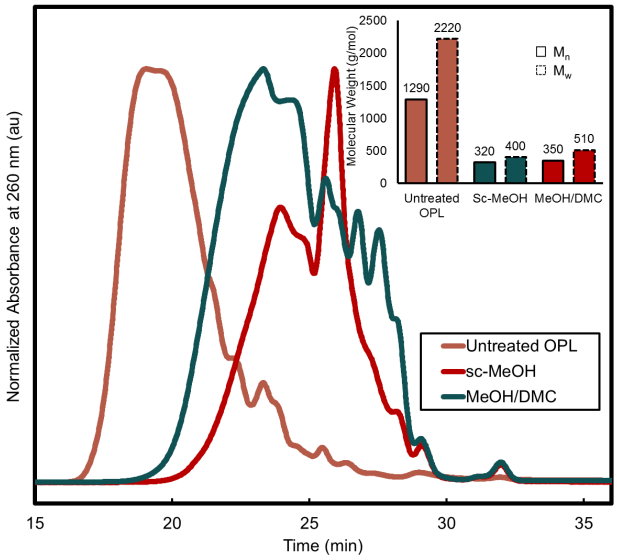

Figure 5. GPC chromatograms for untreated and depolymerized samples. Inset: number average (M_n) and weighted average (M_w) molecular weight for the samples shown.

The decrease in molecular weight can be attributed to solvolytic fragmentation and catalytic HDG of the lignin aryl ether bonds. This is supported by ^{1}H (SI Figures S3 & S4) and 2D ^{1}H-^{13}C HSQC (SI Figure S5) NMR data on the non-volatile products of lignin disassembly with Cu_{20}PMO in sc-MeOH and MeOH/DMC. These data show a large decrease in the chemical shifts associated with both the aliphatic propyl moieties (i.e., β- and γ-carbon) that comprise part of various aryl-ether linkages. The ^{1}H NMR spectra confirmed that the vacuum processing removed the MeOH and DMC, but it is

also likely that some volatile products are removed. Thus, the NMR analyses provides information only about the molecular products with relatively low volatility (e.g., oligomers or small molecules with a low vapor pressure). GC-MS analysis of the liquid nitrogen-trapped solvent and volatile product components removed from the unprocessed products of the 3 h OPL disassembly indicated the minor presence of unidentified compounds (probably aliphatics). Whereas GC-MS analysis of the unprocessed products will detect almost all small molecule compounds (even dimers), it is not capable of oligomer analysis. Therefore, by combining the results of the unprocessed products GC-MS analysis and non-volatile products NMR analysis, a comprehensive snapshot can be developed to describe the chemical and compositional profile of OPL disassembly products.

A quantitative ^{31}P NMR analytical method was used to evaluate the types of free –OH groups that are present in untreated OPL and in the non-volatile products from the catalyzed reactions in sc-MeOH and in MeOH/DMC. This involved phosphorylating the free –OH groups of the samples with 2-chloro-4,4,5,5-tetramethyl-1,3,2-dioxaphospholane (TMDP). The ^{31}P chemical shifts and integration regions for the phosphorylated aryl/alkyl hydroxyl groups were recorded and analyzed by procedures previously used to analyze the hydroxyl functional groups present in lignins and in pyrolysis oils (SI Table S14).[44,45] This quantitative method determines the amounts (mmol) of different types of -OH functional groups per gram of sample. The results of such experiments with untreated OPL and with the non-volatile products from the catalytic disassembly of OPL in sc-MeOH and in MeOH/DMC after 3 h reaction are shown in Figure 6. These data indicate the removal and disruption of the primary and secondary aliphatic alcohols of the alkyl chains linking the aromatic units of lignin. This may result from HDO occurring in conjunction with the HDG disassembly reactions.

Hydrogenolysis of lignin aryl-ether linkages generates phenols, principally the syringyl and guaiacyl terminated fragments (Figure 1). The relatively high content of syringyl units seen in Figure 6 for the disassembly products is consistent with the higher degree of oxygenation in hardwoods such as poplar.[8] For OPL disassembly in the MeOH/DMC co-solvent, lower quantities of syringyl (~142.7 ppm) and guaiacyl (140.2-139.0 ppm) –OH are seen relative to disassembly in sc-MeOH, reflecting partial O-methylation of these species in the co-solvent system. Notably, increased carboxylic acid (136-133.6 ppm) –OH content is seen in the products of catalytically disassembled lignin. The ^{31}P NMR spectra of the products from OPL disassembly in sc-MeOH or MeOH/DMC show no evidence of 5-C substituted or condensed phenolic alcohols, which are formed by recombination of depolymerized compounds. This absence further confirms that Cu_{20}PMO suppresses condensation of reactive intermediates, thus preventing char formation.

^{13}C NMR analyses were also performed on DMSO-d_6 solutions of untreated OPL (Figure 7) and the non-volatile product mixtures from the OPL disassembly in sc-MeOH and in MeOH/DMC (SI Figure S6). This method relies upon the chemical shifts determined by Ben et al.[46] (SI Table S15) to characterize functional group carbons of lignin and pyrolysis oil products.

For the non-volatile products, the ^{13}C NMR spectra (Figure 7) displayed a number of peaks in the 90-0 ppm region indicating the presence of aliphatic carbons. These peaks may indicate the presence of non-volatile aliphatic products as well as alkyl substituents on aromatic lignin fragments. Based on integration of the aliphatic region (excluding DMSO) and of the region assigned to aromatic carbons (160-100 ppm), one can evaluate changes in the nature of the products relative to untreated OPL.

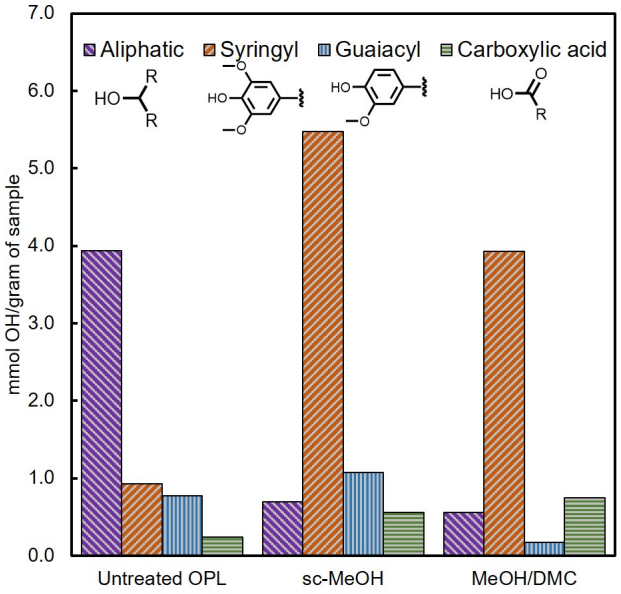

Figure 6. Quantification of the OH functional group content (mmol/g) using the ^{31}P NMR technique with organosolv poplar lignin, and products of OPL disassembly in sc-MeOH, and in MeOH/DMC after 3 h reaction at 300 ^{o}C The bars for each experiment are presented in the order shown at the top.

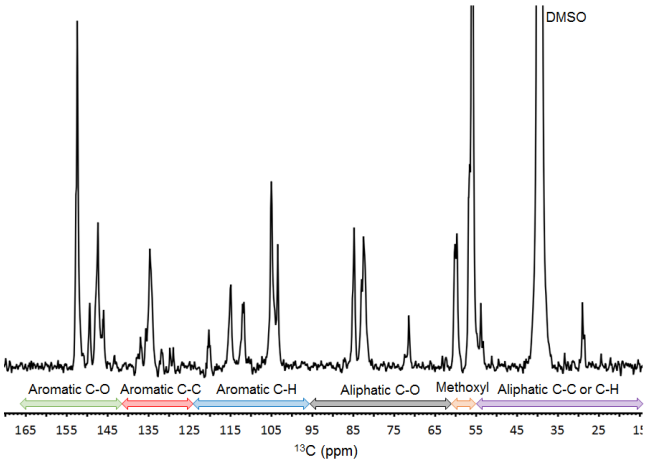

Figure 7. ^{13}C NMR spectrum in DMSO-d_6 of untreated organosolv poplar lignin with peak assignments.

For products generated by OPL disassembly with Cu_{20}PMO in sc-MeOH and in MeOH/DMC, there was a marked reduction in the number of aliphatic carbons adjacent

to an oxygen atom (95.8-60.8 ppm) from about 13% to ~ 1% in both cases (excluding aromatic methoxide groups), an observation clearly consistent with the hydrogenolysis of α-O-4 and β-O-4 ether linkages as well as the HDO of aliphatic alcohols (Figure 8).

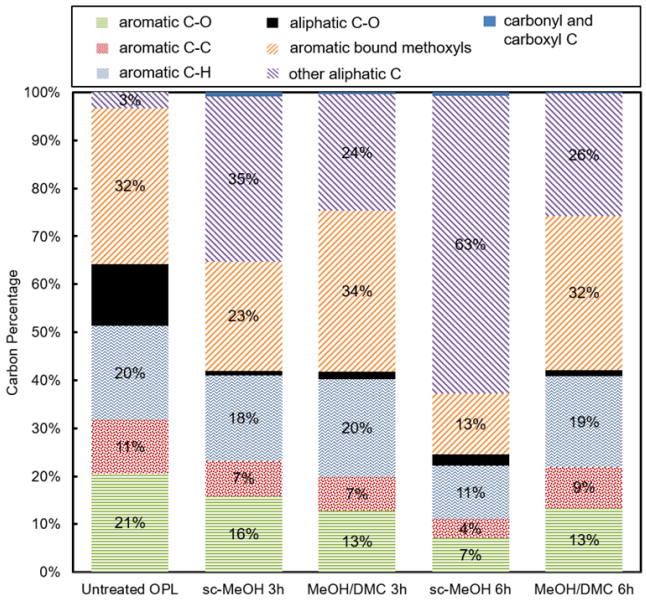

Figure 8. Distribution of carbons (in percent) based on ^{13}C NMR data for untreated OPL and for the products of disassembled OPL in sc-MeOH, and in MeOH/DMC.

Correspondingly, the percentages of aliphatic carbons jumped from 3% in OPL to 32% after 3 h and 63% after 6h reaction in sc-MeOH. In MeOH/DMC aliphatic carbons increased from 3% to 24% after 3 h but this changed little (26%) after 6 h. Another key feature is the reduction in aromatic carbons (C-O at 166.5-142.0 ppm, C-H at 125.0-95.8 ppm and other carbons at 142.0-125.0 ppm) from 51% in OPL to ~42% in the two products after 3 h reaction. In sc-MeOH this continued to decrease to ~23% in the 6 h product, but there was little difference between the compositions of the 3 h and 6 h products in MeOH/DMC. Thus, the reductive disassembly process in both cases is accompanied by some arene hydrogenation. However, the presence of DMC increases the percentage of methoxyl carbons relative to the products generated in sc-MeOH, and such O-methylation stabilizes those products against further hydrogenation. From the model substrate studies and the fact that the aromatic methoxyls (60.8-55.2 ppm) correspond to a much larger percentage of the carbons in the latter product after 3 h, it seems likely that the protective effect involves the O-methylation of phenolate type oxygen.

GC-MS analysis of the unprocessed products from the four lignin disassembly experiments (with/without Cu_{20}PMO and with/without DMC, each for 3 h at 300 ^{o}C) is summarized in SI Table S16. Listed are the major and identified products (>80 % match to the MS database). Heating OPL in these media without catalyst gave liquid fractions with much broader product distributions, in addition to considerable char, than did the Cu_{20}PMO catalyzed disassembly. The 3 h reaction in sc-MeOH with Cu_{20}PMO showed largely phenolic products, whereas analogous methoxybenzene compounds were the principal products in MeOH/DMC.

When studied over a longer reaction time (6 h), the GC-MS data showed that products generated in sc-MeOH demonstrated considerable secondary hydrogenation to aliphatic compounds and significant broadening of the product distribution. In contrast, a narrower distribution was evident from the reaction in MeOH/DMC, and this result can be largely attributed to the methoxybenzene products remaining intact (Figure 9 and SI Figures S7 & S8).

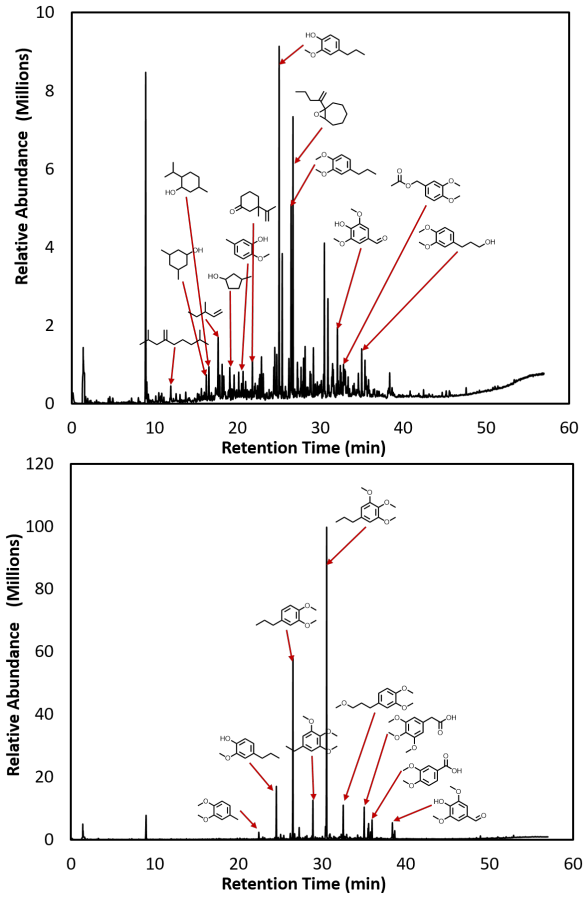

Figure 9. GC-MS chromatograms of liquid products from OPL disassembled by a 6 h reaction with Cu_{20}PMO in sc-MeOH (top) and in MeOH/DMC (bottom). The more abundant components are labeled to illustrate the differences.

In order to study the recyclability of Cu_{20}PMO, the catalyst was recycled in five consecutive 3 h runs, without any regeneration, for OPL reactions in MeOH/DMC. GC-MS analyses of the unprocessed product solutions showed nearly the same yields and compositions for the first three runs (SI Table S17 and Figure S9). However, a significant drop of catalyst activity was observed on the fourth recycle. The nature of this catalysis deactivation and methods for improving recyclability are currently under study.

SUMMARY.

Using select model compounds as a testing platform, these studies indicate that the solvent system can be used to manipu-

late product distribution. The yield of aromatic products from the Cu_{20}PMO catalyzed reductive disassembly of lignin models and of organosolv poplar lignin was substantially increased by the addition of dimethyl carbonate. This strategy exploits the high catalytic activity of copper for hydrogenolysis of aromatic ethers and solid base properties of the PMO support to catalyze O-methylation of phenolic intermediates. Reactive alkylphenols undergo selective O-methylation to form alkylmethoxybenzenes, which are less reactive toward arene hydrogenation, thereby preserving aromaticity and reducing unwanted product proliferation.

While lignin is increasingly used for production of thermoplastics,[47] crosslinkers[48] and carbon materials;[49] its use as an aromatic commodity chemical feedstock is minimal with the exception of vanillin production. The present study represents a clear example of how DMC as a reactive co-solvent can be used to intercept reactive intermediates generated during the reductive disassembly of lignin to give aromatic monomers. The resulting alkylmethoxybenzenes can be used as chemical precursors or can undergo further hydrodeoxygenation to simpler aromatics. Investigations on optimizing the application of such reactive co-solvent systems are currently underway.

ASSOCIATED CONTENT

Supporting Information. The SI is available free of charge on the ACS Publications website at http://pubs.acs.org. The SI contains 34 pp including an expanded description of Experimental procedures for preparation of samples and product analysis of catalyzed reactions, 17 tables, 8 figures and 1 scheme summarizing the detailed results of catalysis runs including additional control reactions for BPE and other model reactions.

AUTHOR INFORMATION

Corresponding Authors

*Email: mfoston@wustl.edu
*Email: ford@chem.ucsb.edu

Author Contributions

‡These authors contributed equally.

Notes

The authors declare no competing financial interests.

ACKNOWLEDGMENT

This research was supported by the National Science Foundation through the Center for Sustainable use of Renewable Feedstocks (CenSURF, NSF CHE-1240194) and by the US Department of Energy Office of Biological and Environmental Research (DE-SC001270). The authors are thankful for the MRL Shared Experimental Facilities, which are supported by the MRSEC Program of the NSF under Award No. DMR 1121053. J.A. Barrett is greatly appreciative of Prof. S. L. Scott of UCSB for providing hydrotalcite and permitting GC-MS usage as well as Lisa Stampler for ATR-FTIR usage.

REFERENCES

(1) U.S. Energy Information Administration. Annual Energy Outlook 2015 http://www.eia.gov/forecasts/aeo.

(2) Wittcoff, H. A.; Reuben, B. G.; Plotkin, J. S. Chapter 4: Chemicals from Natural Gas and Petroleum. In *Industrial Organic Chemicals*; John Wiley & Sons, Inc., 2013; pp 93–138.

(3) Pu, Y. Q.; Zhang, D. C.; Singh, P. M.; Ragauskas, A. J. The new forestry biofuels sector. *Biofuels Bioprod. Bioref.* **2008**, *2*, 58–73.

(4) Ragauskas, A. J.; Williams, C. K.; Davison, B. H.; Britovsek, G.; Cairney, J.; Eckert, C. A.; Frederick Jr., W. J.; Hallett, J. P.; Leak, D. J.; Liotta, C. L.; Mielenz, J.R.; Murphy, R.; Templer, R.; Tschaplinski, T. The Path Forward for Biofuels and Biomaterials. *Science* **2006**, *311*,, 484–489.

(5) Tuck, C. O.; Perez, E.; Horvath, I. T.; Sheldon, R. a.; Poliakoff, M. Valorization of Biomass: Deriving More Value from Waste. *Science* **2012**, *337*, 695–699.

(6) Regalbuto, J. R. Cellulosic Biofuels—Got Gasoline? *Science* **2009**, *325*, 822–824.

(7) Ragauskas, A. J.; Beckham, G. T.; Biddy, M. J.; Chandra, R.; Chen, F.; Davis, M. F.; Davison, B. H.; Dixon, R. A.; Gilna, P.; Keller, M.; Langan, P: Naskar, A. K; Saddler, J. N.; Tschaplinski, T. J.; Tuskan, G. A.; Wyman, C. E. Lignin valorization: improving lignin processing in the biorefinery. *Science* **2014**, *344*, 1246843.

(8) Sannigrahi, P.; Ragauskas, A. J.; Tuskan, G. A. Poplar as a feedstock for biofuels: A review of compositional characteristics. *Biofuels, Bioprod. Biorefining* **2010**, *4*, 209–226.

(9) Argyropoulos, D. S.; Jurasek, L.; Krištofová, L.; Xia, Z.; Sun, Y.; Paluš, E. Abundance and reactivity of dibenzodioxocins in softwood lignin. *J. Agric. Food Chem.* **2002**, *50*, 658–666.

(10) Froass, P. M.; Ragauskas, A. J.; Jiang, J. Chemical Structure of Residual Lignin from Kraft Pulp. *J. Wood Chem. Technol.* **1996**, *16*, 347–365. 0.

(11) Santos, R. B.; Hart, P. W.; Jameel, H.; Chang, H. M. Wood Based Lignin Reactions Important to the Biorefinery and Pulp and Paper Industries. *BioResources* **2013**, *8*, 1456–1477.

(12) Zakzeski, J.; Bruijnincx, P. C. A.; Jongerius, A. L.; Weckhuysen, B. M. The catalytic valorization of lignin for the production of renewable chemicals. *Chem. Rev.* **2010**, *110*, 3552–3599.

(13) Zakzeski, J.; Jongerius, A. L.; Bruijnincx, P. C. A.; Weckhuysen, B. M. Catalytic Lignin Valorization Process for the Production of Aromatic Chemicals and Hydrogen. *ChemSusChem* **2012**, *5*, 1602–1609.

(14) Wang, X.; Rinaldi, R. A Route for Lignin and Bio-Oil Conversion: Dehydroxylation of Phenols into Arenes by Catalytic Tandem Reactions, *Angew. Chem. Int. Ed*. **2013**, *52*, 11499 –11503

(15) Deuss, P. J.; Barta, K. From models to lignin: Transition metal catalysis for selective bond cleavage reactions. *Coord. Chem. Rev.* **2015,** *306*, 510-532.

(16) Barta, K.; Ford, P. C. Catalytic conversion of nonfood woody biomass solids to organic liquids. *Acc. Chem. Res.* **2014**, *47*, 1503–1512.

(17) Parsell, T.; Yohe, S.; Degenstein, J.; Jarrell, T.; Klein, I.; Gencer, E.; Hewetson, B.; Hurt, M.; Kim, J. I.; Choudhari, H.; Saha, B.; Meilan, R.; Mosier, N.; Ribeiro, F.; Delgass, W. N.; Chapple, C.; Kenttamaa, H.I.; Agrawal, R.; Abu-Omar, M. M. A synergistic biorefinery based on catalytic conversion of lignin prior to cellulose starting from lignocellulosic biomass. *Green Chem.* **2015**, *17*, 1492–1499.

(18) Parsell, T. H.; Owen, B. C.; Klein, I.; Jarrell, T. M.; Marcum, C. L.; Haupert, L. J.; Amundson, L. M.; Kentt, H. I.; Ribeiro, F.; Miller, J. T.; Abu-Omar, M. M. Cleavage and hydrodeoxygenation (HDO) of C–O bonds relevant to lignin conversion using Pd/Zn synergistic catalysis. *Chem. Sci*., **2013**, *4*, 806-813

(19) Zaheer, M.; Kempe, R. Catalytic Hydrogenolysis of Aryl Ethers: A Key Step in Lignin Valorization to Valuable Chemicals. *ACS Catal.* **2015**, *5*, 1675−1684.

(20) Sinfelt, J. H. Catalytic hydrogenolysis on metals. *Catal. Letters* **1991**, *9*, 159–172.

(21) Kim, S.; Chmely, S. C.; Nimlos, M. R.; Bomble, Y. J.; Foust, T. D.; Paton, R. S.; Beckham, G. T. Computational study of bond dissociation enthalpies for a large range of native and modified Lignins. *J. Phys. Chem. Lett.* **2011**, *2*, 2846–2852.

(22) Song, Q.; Wang, F.; Xu, J. Hydrogenolysis of lignosulfonate into phenols over heterogeneous nickel catalysts. *Chem. Commun.* **2012**, *48*, 7019–7021.

(23) Song, Q.; Wang, F.; Cai, J.; Wang, Y.; Zhang, J.; Yu, W.; Xu, J. Lignin depolymerization (LDP) in alcohol over nickel-based catalysts via a fragmentation-hydrogenolysis process. *Energy Environ. Sci.* **2013**, *6*,

994–1007.
(24) Macala, G. S.; Matson, T. D.; Johnson, C. L.; Lewis, R. S.; Iretskii, A. V.; Ford, P. C. Hydrogen transfer from supercritical methanol over a solid base catalyst: A model for lignin depolymerization. *ChemSusChem* **2009**, *2*, 215–217.
(25) Macala, G. S.; Robertson, A. W.; Johnson, C. L.; Day, Z. B. Lewis, R. S.; White, M. G.; Iretskii, A. V.; Ford, P. C. Transesterification catalysts from iron doped hydrotalcite-like precursors. Solid Bases for Biodiesel Production, *Catal. Let.* **2008**, *122*, 205-209.
(26) Matson, T. D.; Barta, K.; Iretskii, A. V; Ford, P. C. One-pot catalytic conversion of cellulose and of woody biomass solids to liquid fuels. *J. Am. Chem. Soc.* **2011**, *133*, 14090–14097.
(27) Barta, K.; Matson, T. D.; Fettig, M. L. Scott, S. L.; Iretskii, A. V.; Ford, P. C. Catalytic disassembly of organosolv lignin via hydrogen transfer from supercritical methanol, *Green Chem.* **2010**, *12*, 1640-7.
(28) Barta, K.; Warner, G. R.; Beach, E. S.; Anastas, P. T. Depolymerization of organosolv lignin to aromatic compounds over Cu-doped porous metal oxides. *Green Chem.* **2014**, *16*, 191–196.
(29) Huang, X.; Korányi, T. I.; Boot, M. D.; Hensen, E. J. M. Catalytic depolymerization of lignin in supercritical ethanol. *ChemSusChem* **2014**, *7*, 2276–2288.
(30) Huang, X.; Atay, C.; Korányi, T. I.; Boot, M. D.; Hensen, E. J. M. Role of Cu–Mg–Al Mixed Oxide Catalysts in Lignin Depolymerization in Supercritical Ethanol. *ACS Catal.* **2015**, *5*, 7359–7370.
(31) Sun, Z.; Bottari, G.;. Barta, K. Supercritical methanol as solvent and carbon source in the catalytic conversion of 1,2-diaminobenzenes and 2-nitroanilines to benzimidazoles. *Green Chem.* **2015,** *17*, 5172-5181.
(32) Hansen, T. S.; Barta, K.; Anastas, P. T.; Ford, P. C.; Riisager, A. One-pot reduction of 5-hydroxymethylfurfural via hydrogen transfer from supercritical methanol. *Green Chem.* **2012**, *14*, 2457–2461.
(33) Bernt, C. M.; Bottari, G.; Barrett, J. A.; Scott, S. L.; Barta, K.; Ford, P. C. Mapping reactivities of aromatic models with a lignin disassembly catalyst. Steps toward controlling product selecivity. *Catal. Sci. Technol.* **2016**, *6*, 2984-94.
(34) Talawar, M. B.; Jyothi, T. M.; Raja, T.; Rao, B. S.; Sawant, P. D. Calcined Mg–Al hydrotalcite as an efficient catalyst for the synthesis of guaiacol. *Green Chem.* **2000**, *2*, 266–268.
(35) Jyothi, T. M.; Raja, T.; Talawar, M. B.; Sugunan, S.; Rao, B. S.; Energy, H. Selective Methylation of Phenol, Aniline and Catechol with Dimethyl Carbonate Over Calcined Mg-Al Hydrotalcites. *Synth. Commun.* **2000**, *30*, 3929–3934.
(36) Nichols, J. M.; Bishop, L. M.; Bergman, R. G.; Ellman, J. A. Catalytic C - O Bond Cleavage of 2-Aryloxy-1-arylethanols and Its Application to the Depolymerization of Lignin-Related Polymers. *J. Am. Chem. Soc.* **2010**, *132*, 12554–12555.
(37) Kleineri, T. N. Organosolv Pulping and Recovery Process. US 3,585,104, 1971.
(38) Downs, R. T.; Hall-Wallace, M. The American Mineralogist crystal structure database. *Am. Mineral.* **2003**, *88*, 247–250.
(39) Scanlon, J. T.; Willis, D. E. Calculation of Flame Ionization Detector Relative Response Factors Using the Effective Carbon Number Concept. *J. Chromatogr. Sci.* **1985**, *23*, 333–340.
(40) Kuzmic, P. Program DYNAFIT for the analysis of enzyme kinetic data: application to HIV proteinase. *Anal. Biochem.* **1996**, *237*, 260–273.
(41) Popov, A.; Kondratieva, E.; Goupil, J. M.; Mariey, L.; Bazin, P.; Gilson, J. P.; Travert, A.; Maugé, F. Bio-oils hydrodeoxygenation: Adsorption of phenolic molecules on oxidic catalyst supports. *J. Phys. Chem. C* **2010**, *114*, 15661–15670.
(42) Chui, M.; Metzger, G; Azumi, T; Bernt, C; Tran, A.; Boscolo, M; Ford, P.C. Presented at the 251st National Meeting of the American Chemical Society, San Diego, CA, March 13-17, 2016; Poster CATL 256.
(43) Pandey, M. P.; Kim, C. S. Lignin Depolymerization and Conversion: A Review of Thermochemical Methods. *Chem. Eng. Technol.* **2011**, *34*, 29–41.
(44) Pu, Y.; Cao, S.; Ragauskas, A. J. Application of quantitative 31P NMR in biomass lignin and biofuel precursors characterization. *Energy Environ. Sci.* **2011**, *4*, 3154-3166.
(45) Ben, H.; Ragauskas, A. J. Pyrolysis of kraft lignin with additives. *Energy and Fuels* **2011**, *25*, 4662–4668. DOI: 10.1021/ef2007613.
(46) Ben, H.; Ragauskas, A. J. NMR characterization of pyrolysis oils from kraft lignin. *Energy and Fuels* **2011**, *25*, 2322–2332.
(47) Sadeghifar, H.; Cui, C.; Argyropoulos, D. S. Toward Thermoplastic Lignin Polymers. Part 1. Selective Masking of Phenolic Hydroxyl Groups in Kraft Lignins via Methylation and Oxypropylation Chemistries. *Ind. Eng. Chem. Res.* **2012**, *51*, 16713–16720.
(48) Sen, S.; Patil, S.; Argyropoulos, D. S. Methylation of softwood kraft lignin with dimethyl carbonate. *Green Chem.* **2015**, *17*, 1077–1087.
(49) Oroumei, A.; Fox, B.; Naebe, M. Thermal and Rheological Characteristics of Biobased Carbon Fiber Precursor Derived from Low Molecular Weight Organosolv Lignin. *ACS Sustainable Chem. Eng.* **2015**, *3*, 758–769.

Table of Contents Illustration:

Enhancing Aromatic Production from Reductive Lignin Disassembly: *in situ* O-methylation of Phenolic Intermediates.

Jacob A. Barrett, Yu Gao, Christopher M. Bernt, Megan Chui, Anthony T. Tran, Marcus B. Foston*, Peter. C. Ford*.

Synopsis: Dimethyl carbonate added to a catalytic system that uses Cu_{20}PMO in sc-MeOH to disassemble biomass lignin enhances yields of aromatics.